

Residual Solvent Effects on Free Volume and Performance of Fluorinated Polyimide Membranes: A Molecular Simulation Study

Kai-Shiun Chang, Chi-Chung Hsiung, Chih-Cheng Lin, and Kuo-Lun Tung*

R&D Center for Membrane Technology and Department of Chemical Engineering,
Chung Yuan Christian University, Chung-Li, Taoyuan 320, Taiwan

Received: January 10, 2009; Revised Manuscript Received: March 1, 2009

In this study, molecular simulation techniques were used to investigate the residual solvent effects on the free volume and performance of 6FDA-mPDA polyimide (PI) membranes. A molecular dynamics (MD) simulation was used to analyze how the residual solvent in the 6FDA-mPDA PI membrane affects the fluctuation and flexibility of the polymer segment and the free volume. The gas sorption in the membrane was analyzed by a Monte Carlo (MC) technique. The energy analysis of the MD simulation indicates that the presence of solvent molecules tends to favor the fluctuation, and flexibility of polymer segments tended to be encouraged due to the presence of solvent molecules through the energy analysis by MD simulation. The free volume analysis revealed that the free space in the membrane would be enlarged by extracting the solvent from the membrane. The gas sorption behavior, analyzed by the MC technique, showed that gas solubility increased in the lower residual solvent membranes. This was caused by the free volume released by extracting the solvent, thus providing more suitable sites for gas sorption. The sorption ability was also affected by the intermolecular attractive energy, while the free volumes inside the membranes were similar. In addition, the residual solvent effect on gas sorption would be eliminated at higher pressure. From the thermal motion analysis of gas molecules, it was found that the effective thermal motion of gaseous molecules improved as residual solvent molecules remained in the membrane matrix, but this did not have an effective influence on gas permeation.

1. Introduction

The membrane technique of gas separation has become one of the major industrial applications of membrane technology over the past 20 years.¹ One of the major methods of preparing membranes for gas separation is the phase inversion method. However, the complicated physical properties of the casting solvents selected may affect the mechanism of membrane fabrication, forming membranes with different characteristics. The effects of solvent types on the free volume and performance of membranes have been discussed in previous reports. In these studies, it was pointed out that the casting solvent had an important role in determining the free volume morphology, crystalline structure, and polymer flexibility of the membrane. Meanwhile, gas transport behaviors, including sorption, diffusion, and permeation, were also obviously affected.^{2–6}

In the phase inversion method, high temperature treatment with a vacuum environment is used to remove the casting solvent remaining inside of the membrane. However, solvent molecules cannot be removed entirely, and even a small amount of residual solvent might have a strong influence on the membrane.⁷ As a result, the solvent remaining in the membrane after the preparation process might be one of the factors that govern its characteristics and gas transport behavior. Several previous studies have reported the effects of the residual solvent on the membrane structure and its separation performance.^{8–13}

For example, Brown et al.⁸ prepared the polysulphone hollow fiber membrane under cold water, hot water, and vacuum treatment to leave different quantities of solvent in the membrane. It was pointed out that the percentage of residual solvent

and surface morphology would be changed through these heat treatments. In their study, it was presumed that the removal of residual solvent from the selective layer was the crucial factor determining the separation ability. Sakaguchi et al.⁹ extracted the residual solvent in the poly(sulfone-amide) membrane by different annealing temperatures. They suggested that the polymer chains would be more easily rearranged at relatively low temperatures in the as-cast membrane. Meanwhile, the residual stress might cause a uniform densification phenomenon. On the other hand, the densification was not uniform in the extracted membrane, which then had more defects that accelerated the diffusivity of gas molecules. Leblanc et al.¹⁰ reported that the characteristics of dense membranes, such as the 6FDA-mPDA polyimide membrane, highly depended on the nature of the solvent and that the permeation properties were dominated by the presence of residual solvent. However, membrane curing was believed to eliminate the effect of casting solvent due to the reorganization of the polymer chains. Moe et al.¹¹ discussed the effect of film history on fluorinated aromatic polyimide membranes. Depending on this history, various amounts of DMAc solvent would remain in the as-cast and annealed membranes. An apparent difference between the helium and carbon dioxide permeability of the as-cast and annealed membranes was observed, and antiplasticization, which was caused by residual solvent and aging effects, was cited as a possible factor. They recognized that solvent molecules in the membranes might play the role of antiplasticizers, which would stiffen the polymer chains and retard segment motion. These effects would consequently reduce gas permeation compared to solvent-free polymeric membranes. Fu et al.¹² reported that motion of polymer segments was promoted by residual solvent,

* Address all correspondence to the following: telephone, +886-3-2654129; fax, +886-3-2654199; e-mail, kuolun@cycu.edu.tw.

which played the role of a plasticizer as long as it remained in the membrane. This plasticization enlarged the free volume and increased gas permeation. Moreover, the action of the residual solvent switched from plasticization to antiplasticization when the solvent percentage fell below a critical value. Joly et al.¹³ investigated the residual solvent effect on 6FDA-mPDA membranes fabricated by five different casting solvents using various thermal treatment times. Their work showed that polymer plasticization due to solvent molecules lowered the glass transition temperature of the membrane and also raised its gas diffusivity. On the other hand, solubility was clearly reduced by sorption site competition between solvent and gas molecules, which ultimately leads to lower permeability. From the past reports we mentioned above, residual solvent was regarded as a plasticizer, and whether it acted as an antiplasticizer in the polymer matrix remained unclear due to complicating factors in the fabrication process and molecular-scale interactions between the polymer, casting solvent, and gas molecules. Meanwhile, totally residual solvent removal could only be ensured by annealing the polymer above its glass transition temperature.⁵ Hence, there is still some difficulty in accurately controlling the amount of residual solvent experimentally.

The molecular dynamics technique is a potential method of gaining insight into polymeric membrane characteristics, including polymer configuration, free volume, and transport behaviors on the microscopic scale.^{14–27} Smit et al.¹⁴ analyzed the diffusion mechanisms of small molecules in the polyimide membrane via a molecular dynamics (MD) simulation. Two different types of diffusion behavior, residual time and flying time, were observed. Gee et al.¹⁵ pointed out that raising the temperature would improve small molecule thermal motion and thus contribute to an increase in diffusivity by raising the temperature. At the same time, more free volume could be obtained at higher temperatures. From past studies,^{16–18} the free volume distribution was also analyzed by the molecular simulation technique and positron annihilation lifetime spectroscopy (PALS). There is good agreement between the results obtained from theoretical and experimental work. In the simulation,^{17,18} two methods of free volume analysis, V_connect and R_max, were used to simulate the free volume distribution of membranes caused by various backbone stiffnesses and substituent types. In addition, the relationships among polymer structure, free volume, and gas transport behavior from the calculations were also discussed and then compared with the PALS results. Tung et al.¹⁹ investigated the effect of the tacticity of PMMA on the free volume and gas transport behavior of the membrane using MD and Monte Carlo (MC) techniques. Moreover, the effects of casting solvent types on free volume morphology and the gas transport mechanism were analyzed, and the results obtained were in good agreement with the experimental data.^{20,21} Furthermore, the viewpoint of energy analysis was adopted to probe the free volume instead of the conventional geometrical analysis, and this approach also yielded results in good agreement with experimental data.^{22,23}

However, to the best knowledge of the authors, the residual solvent effect on the 6FDA-mPDA polyimide membrane has not been investigated using the molecular simulation technique. An in-depth analysis at the molecular scale is necessary for further understanding to obtain much more useful information and to gain much better performance. Hence, we adopted the molecular simulation technique to investigate the effects of residual solvent on the 6FDA-mPDA polyimide membrane by molecular simulation techniques for gaining the insight understanding. The reason for selecting the 6FDA-mPDA polyimide

membrane was due to its excellent chemical and thermal properties, that were reported to be widely used in the field of gas separation. In addition, the 6FDA-based polyimide membrane contained bulky CF₃ groups which donated higher permeability and selection factor for gas separation, such as carbon dioxide separation.^{13,28–31} Furthermore, previous reports also pointed out the 6FDA-based polyimide membranes have high potential to exceed the “upper bound” trade-off line. As a result, an analysis at a molecular scale is helpful for understanding the mechanism of high performance behavior of the 6FDA-based polyimide membranes and is a benefit to design new polymeric materials for crossing this “upper bound” trade-off line boundary.^{25,32–35}

In this study, the membrane structure, free volume, and diffusion mechanism were analyzed via an MD technique. Gas sorption behaviors were analyzed using the MC technique. To confirm the accuracy of the simulation, the calculation results in this study were compared with experimental data from the report of Joly et al.¹³ on the residual solvent effect on 6FDA-mPDA polyimide membranes.

2. Theoretical Method

This study investigated the residual solvent effect on the 6FDA-mPDA polyimide (PI) membrane. All the PI membrane models were built using the *Cerius²* package provided by Accelrys (originally MSI). All the queuing calculations were performed on the SGI Origin 3800 and SGI 2000 high performance computers at the National Center for High-Performance Computing (NCHC), Taiwan. Both the physical membrane properties for the molecular models constructed in this study and the experimental data used for comparison were obtained from the results of Joly et al.¹³ The details of constructing the PI membrane models are described below.

2.1. Construction of 6FDA-mPDA PI Membrane Models. In this study, five kinds of solvents were chosen to construct the membrane-solvent solution models: N-methyl-2-pyrrolidone (NMP), N,N-dimethyl acetamide (DMA), dioxane (DIO), tetrahydrofuran (THF), and dichloromethane (DIC), ordered by their boiling points, from highest to lowest. The different percentages of solvent (by weight) remaining in the membrane after various thermal treatment times could be determined by TGA analysis from the report of Joly et al.¹³ Meanwhile, it was assumed that the weight loss in the membrane that occurred after the annealing process was only caused by the residual evaporation because no chemical reaction occurred during the thermal treatment. Hence, the different solvent quantities remaining in the membrane could be controlled by the different thermal treatment times at 120 °C under vacuum, either 2880 or 90 min. The membrane models we built in this study were named PI_2880_NMP, PI_2880_DMA, PI_2880_DIO, PI_2880_THF, PI_2880_DIC, PI_90_NMP, PI_90_DMA, PI_90_DIO, PI_90_THF, and PI_90_DIC, according to the thermal treatment times and selected solvents, respectively. As expected, the PI_90 series membranes contained more solvent than the PI_2880 series membranes.

Table 1 lists the membrane weight loss and construction parameters, where the weight loss data was taken from ref 13. The membrane models with different amounts of solvent were built in three steps. First, five membrane solution models containing 6FDA-mPDA polyimide chains and various solvents were built by energy minimization over 1000 iterations using the COMPASS force field to obtain the stable structures. All the 6FDA-mPDA polyimide membranes cast from different solvents and processed by long-term annealing were regarded

TABLE 1: Parameters Used in the PI Membrane Models

casting solvent	T_{bp}^b (°C)	wt loss ^a (wt %)		model parameter		no. of solvent molecules		
		90 min	2880 min	monomers	chains	initial	90 min	2880 min
NMP	197	4.5	1.24	23	2	50	11	3
DMAc	165	4.5	0.95	18	2	50	10	2
dioxane	101	6.5	1.00	24	2	50	19	3
THF	66	2.5	0.71	20	2	50	7	2
dichloromethane	40	1.5	0.57	16	2	50	3	1

^a From Joly et al.¹³ ^b T_{bp} : the boiling point.

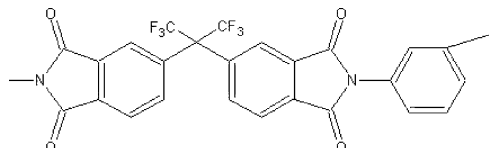


Figure 1. Primary structure of 6FDA-mPDA polyimide.

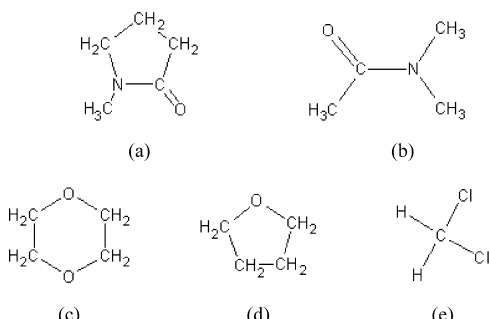


Figure 2. Schematic presentation of structures of solvents used in membrane–solvent solution: (a) *N*-methyl-2-pyrrolidone (NMP); (b) *N,N*-dimethyl acetamide (DMAc); (c) dioxane (DIO); (d) tetrahydrofuran (THF); (e) dichloromethane (DIC).

as solvent-free, and their densities were all taken to be 1.45 g/cm³, as per ref 13. As a result, the densities of the solvent-free membrane models in our work were set to 1.45 g/cm³. Meanwhile, the densities of membrane–solvent solutions were obtained by calculation with the densities of selected solvents and solvent free membranes. The polymer monomer and solvent structure are shown in Figures 1 and 2. The molecular model parameters of the solution are listed in Table 1, and the physical properties of the solvents and the solution are illustrated in Table 2. Next, the second step is the solvent evaporating stage. The solvent molecules were chosen randomly to be removed at three time points to imitate the evaporation states. Moreover, the energy minimization was repeated each time after solvent was removed from those solutions. It was assumed that the solvent evaporated from the membranes rapidly during the process, and the small quantity of molecules would not affect the polymer structure. Finally, the number of solvent molecules remaining in the solution was fixed to match the experimental data, giving the same percentage of residual solvent (by weight). The energy minimization was carried out to get the ultimate stable membrane models. After that, a 50 ps MD calculation was performed under the NVT ($T = 308$ K) ensemble condition to equilibrate the matrix. Then, the MD simulation was carried out under the same conditions for a duration of 1 ns, with a time step of 1 fs, to analyze the membrane structure, the polymer properties, and the gas diffusion mechanism. Later, the gas sorption behavior was explored by MC simulation.

2.2. COMPASS Force Field. The COMPASS force field (condensed-phase optimized molecular potential for atomistic simulation studies) was used in this study for the theoretical calculations. The energy terms were divided to three sections:

the bonded energy terms, the cross-terms, and the nonbonded energy terms. The bonded energy terms consisted of (a) the covalent bond stretching energy terms, (b) the bond angle bending energy terms, and (c) the torsion angle rotation energy terms of the polymer chain. The energy of the torsion angle was fitted by a Fourier series function. The out-of-plane energy, or improper term (d), is described as a harmonic function. The terms of cross interaction include the dynamic variation among the bond stretching, bending, and torsion angle rotation (e–j). The last two terms, k and l, represent the Coulombic electrostatic force and van der Waals force, respectively, which are interactive forces between polymer chains and solvent molecules.

$$\begin{aligned}
 E = & \sum_b \left[K_2(b - b_0)^2 + K_3(b - b_0)^3 + K_4(b - b_0)^4 \right] \\
 & \quad \text{(a)} \\
 & + \sum_\theta \left[H_2(\theta - \theta_0)^2 + H_3(\theta - \theta_0)^3 + H_4(\theta - \theta_0)^4 \right] \\
 & \quad \text{(b)} \\
 & + \sum_\phi \left[V_1[1 - \cos(\phi - \phi_0)] + V_2[1 - \cos(2\phi - \phi_2)] + V_3[1 - \cos(3\phi - \phi_3)] \right] \\
 & \quad \text{(c)} \\
 & + \sum_x K_x x^2 + \sum_b \sum_{b'} F_{bb'}(b - b_0)(b' - b'_0) + \sum_\theta \sum_{\theta'} F_{\theta\theta'}(\theta - \theta_0)(\theta' - \theta'_0) \\
 & \quad \text{(d)} \qquad \text{(e)} \qquad \text{(f)} \\
 & + \sum_b \sum_\theta F_{b\theta}(b - b_0)(\theta - \theta_0) + \sum_b \sum_\phi (b - b_0)[V_1 \cos \phi + V_2 \cos 2\phi + V_3 \cos 3\phi] \\
 & \quad \text{(g)} \qquad \text{(h)} \\
 & + \sum_{b'} \sum_\phi (b' - b'_0)[V_1 \cos \phi + V_2 \cos 2\phi + V_3 \cos 3\phi] \\
 & \quad \text{(i)} \\
 & + \sum_\phi \sum_{\theta'} \sum_{\theta''} K_{\phi\theta\theta''} \cos \phi(\theta - \theta_0)(\theta' - \theta'_0) + \sum_{ij} \frac{q_i q_j}{\sigma r_{ij}} + \sum_{ij} \left[2 \left(\frac{A_{ij}}{r_{ij}^9} \right) - 3 \left(\frac{B_{ij}}{r_{ij}^6} \right) \right]
 \end{aligned} \quad \text{(1)}$$

2.3. Physical Property Analysis. Radial Distribution Function (RDF). The radial distribution function (RDF) was the main tool adopted to analyze the microstructure of the material. This function counts the number of two-atom species with specific distances, and it is defined as

$$g_{\alpha\beta}(r) = \frac{V_0}{N_\beta 4\pi r^2 \Delta r} \frac{N_{\beta(r)}}{N_{\beta(r)}} \quad \text{(2)}$$

where V_0 is the cell volume, N_β is the total number of β atoms, and $N_{\beta(r)}$ is the number of β atoms found within a spherical shell of r to $r + \Delta r$ corresponding to α atoms.

Fractional Free Volume. The fractional free volume (FFV) and van der Waals Volume (V_W) are obtained by the following equations:

$$\text{FFV} = \frac{V - V_0}{V} \quad \text{(3)}$$

$$V_0 = 1.3V_W \quad (4)$$

where V_W was obtained from the van der Waals surface instead of using the Bondi's groups. The accessible volume and fractional accessible volume (FAV) were calculated by the hard spherical particle to probe the volume that was available for a particle passing through. The free volume morphology could be obtained by analyzing the cross sections of the cubic membrane model in the x , y , and z directions. The image of the cross section was treated as a graph composed of 256 pixels \times 256 pixels. The areas occupied by the free volume in the cross section were calculated and transformed to the equivalent diameters. Then, the free volume size distribution was obtained by counting the free volume equivalent diameters.

Sorption and Diffusion Mechanisms. The sorption process of gaseous molecules with a membrane includes (1) the molecule is absorbed in the membrane matrix, (2) the absorbate reacts or exchanges sorption position in the membrane matrix, and (3) the absorbate desorbs from the membrane matrix. To calculate and illustrate the three sorption mechanisms correctly, the Monte Carlo simulation was used in our present work. In this study, the grand canonical Monte Carlo method (GCMC) was utilized to simulate the sorption interface behaviors, and the gas concentration probability in the membrane matrix could be determined by the energy change between the new configuration and the previous one. In this procedure, the Metropolis algorithm was used to decide the acceptance or rejection of the configurational moving of sorbate molecules. There are four types of configurational moving, including configuration creation, configuration rotation, configuration translation, and configuration destruction. The creation and destruction probabilities of the movements of sorbate molecules can be expressed as

$$P = \min \left[1; \exp \left(-\frac{\Delta E}{kT} \pm \ln \frac{(N_i + 1)kT}{f_i V} \right) \right] \quad (5)$$

where ΔE is the energy change between the new configuration and the previous one, k is Boltzmann's constant, T is the assigned simulation temperature, N_i is the number of component i molecules in the configuration, f is the fugacity of the component i molecule, and V is the cell volume. The probability of translational movement in the membrane cell is

$$P = \min \left[1; \exp \left(-\frac{\Delta E}{kT} \right) \right] \quad (6)$$

All four kinds of the aforementioned probabilities were calculated and considered as a completed Monte Carlo calculation step. The sorption analysis calculation in this study was processed 1,000,000 times. The number of sorption configura-

tions accepted was recorded and calculated as the sorption concentration and loading.

The gas diffusion mechanism in the membrane could be classified into thermal jumping, diffusive motion, and trapped motion, respectively. The classification was mainly decided by the average radius or diameter of the atoms, as calculated from their van der Waals volume in the membrane. The diffusion mechanism of gas molecules was classified as thermal jumping if the value of its mean-squared distance (MSD) was larger than the average radius (R_{eq}^2) or the average diameter (D_{eq}^2) during the specific time duration, where the average radius and diameter could be expressed as

$$R_{eq} = \left(\frac{3}{4} \frac{\sum_{i=1}^n V_{w,i}}{n\pi} \right)^{1/3} \quad \text{and} \quad D_{eq} = 2 \left(\frac{3}{4} \frac{\sum_{i=1}^n V_{w,i}}{n\pi} \right)^{1/3} \quad (7)$$

To analyze the diffusive mechanism, the slope of the five continuous MSD values could be calculated using the least-squares method. The mechanism was considered to be of diffusive type if the value of the slope was less than 0.5. Finally, the probability of the trapped mechanism was obtained by subtracting the probabilities of the thermal jumping and diffusive mechanisms from unity.

3. Results and Discussion

3.1. Validation of the Molecular Models. We calculated the solubility coefficients of gases on the membrane models that were built by molecular mechanics in our initial step. This was used to validate whether the molecular model was suitable to analyze the residual solvent effect. We could confidently confirm that the simulation method in our study was able to reveal the influence of residual solvent if there was a clear difference in the sorption loading from the membranes with different quantities of solvent inside.

Figure 3 illustrates the residual solvent effect on the N_2 and CO_2 solubility coefficients on the five kinds of PI membranes. It was found that the gas solubility coefficients increased when the PI membranes contained less residual solvent. This might be caused by the sorption site competition between gas and solvent molecules.¹³ In addition, there was an obvious difference between the sorption ability of the N_2 and CO_2 , which was apparent by comparing their solubility coefficients. As a result, it was suggested that the models built in this study could describe the sorption abilities of various gases. Moreover, we found similar results of the gas sorption behaviors (both of N_2 and CO_2) we mentioned above under different operation pressures from 1 to 10 bar. The sorption isotherms of PI_90 and PI_2880 series membranes approached each other when the variation of the residual solvent quantity between them decreased (where the ordering of the residual solvent differences was DIO > DMA).

TABLE 2: Physical Properties of Various Solvents and Membrane Parameters Used in This Work

solution	casting solvent	MW ^b	$\rho_{solvent}^c$ (g/cm ³)	molar volume (cm ³ /mol)	$\rho_{membrane}^a$ (g/cm ³)	
					90 min	2880 min
PI_NMP	<i>N</i> -methyl-2-pyrrolidone	99	1.0270	96.39	1.5165	1.4681
PI_DMA	<i>N,N</i> -dimethyl acetamide	87	0.9366	92.89	1.5179	1.4636
PI_DIO	dioxane	88	1.0328	85.19	1.5749	1.4720
PI_THF	tetrahydrofuran	72	1.1261	81.08	1.4854	1.4601
PI_DIC	dichloromethane	85	1.3660	63.62	1.4724	1.4575

^a $\rho_{membrane}$: the density of the 6FDA-mPDA polyimide membrane. ^b MW: the molecular weight. ^c $\rho_{solvent}$: the density of the casting solvent.

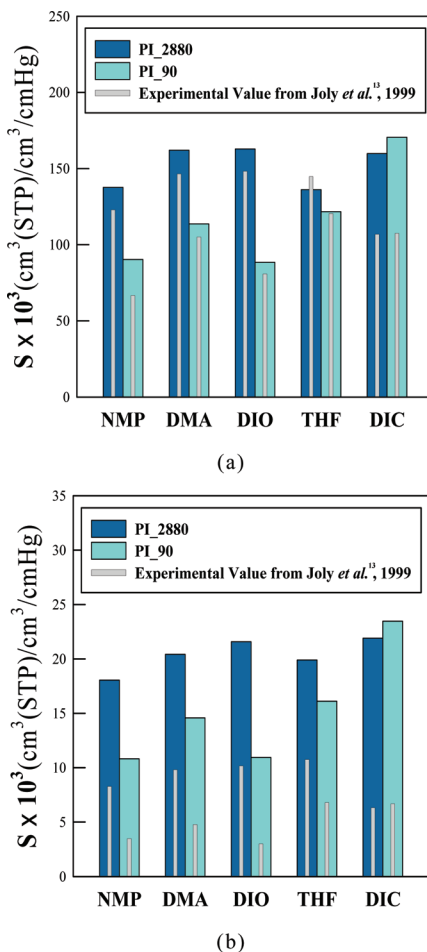


Figure 3. Solubility coefficients for model validation of (a) N_2 and (b) CO_2 on 6FDA-mPDA polyimide membranes cast from various casting solvents.

> NMP > THF > DIC), although we do not graph the isotherms here. This indicates that the gas sorption is controlled by the solvent molecules in the membrane. A similar result appears in our MD analysis, which will be discussed in the following section. These simulated results are also in close agreement with the experimental data.¹³ Hence, it was confirmed that the residual solvent effect can be expressed by the molecular models constructed in this study. Afterward, an MD simulation of 1000 ps duration was performed to analyze the membrane properties and gas transport mechanisms, including sorption and diffusion, as in the following discussion.

3.2. Effect of Residual Solvent on Membrane Structure. **Energy Analysis of the Membrane Matrix.** The glass transition temperature (T_g) is one of the important parameters in polymer structure analysis. The variance of T_g indicates the change of polymer chain structure and its properties, such as flexibility or stiffness. Joly et al.¹³ measured the T_g of 6FDA-mPDA polyimide membranes cast from NMP that annealed for 2880 and 90 min, respectively. It was found that the T_g decreased from 307 to 304 °C when there was about 4.5 wt % residual NMP in the membrane compared with the solvent-free membrane. It was considered that the intermolecular attractive interaction might be reduced, and then the polymer flexibility would be increased when the solvent molecules remained in the membrane. Thus, the energy analysis of polymer chains was carried out in order to compute the intermolecular, intramolecular, and total energy of the polymer matrix. Table 3 lists the energy terms of five kinds of PI membranes containing

various quantities of residual solvent. It shows that, when the number of solvent molecules in the membrane decreased, the intermolecular attractive energy (negative value) was improved, and the intramolecular repulsive energy (positive value) was reduced. As a result, the repulsive force inside the membranes tended to increase as higher quantities of solvent remained in the PI membrane, and this in turn promoted the polymer fluctuations. Figure 4 shows the kinetic energy of molecules in different PI membranes. It shows that the kinetic energy is relatively higher in the PI_90 series membranes, which contain more residual solvent inside. Therefore, it was considered that the fluctuation and flexibility of chains were likely promoted by the presence of solvent molecules in the membrane. Furthermore, it was also found that the energy differences (Coulombic force and kinetic energy) between the PI_90 and PI_2880 series membranes could be ordered as follows: PI_DIO > PI_NMP > PI_DMA > PI_THF > PI_DIC. On the other hand, we could probably calculate the values of the released free volume between PI_90 and PI_2880 membranes by multiplying the values of solvent molecule volume and their quantity differences. The tendency of probably released volume is identical with the difference of energy we mentioned above. Hence, it was hypothesized that the residual solvent effect on the molecular energy was mainly controlled by the molar volume and the quantity of residual solvent.

Radial Distribution Function (RDF) of Polymer Chains. To discuss the effect of residual solvent on the polymeric structure, the radial distribution function (RDF) of the carbon atom with itself in the PI_2880_NMP and PI_90_NMP membranes was analyzed, as shown in Figure 5a. In Figure 5a, the RDFs of C and C atoms almost overlap. This overlap indicates that the structures of the main polymer chains were mainly controlled by the nature of the material (6FDA-mPDA polyimide), and the quantity of solvent did not have much influence on the main structure. But some characteristics were clearly found to change between the PI_2880 and PI_90 series membranes, such as the attractive energy and kinetic energy mentioned above. Figure 5b illustrates the RDF of atom pairs on the side chains of PI_2880_NMP and PI_90_NMP membranes. By comparing the peaks of PI_90_NMP with the PI_2880_NMP membrane, we found that there are two broader peaks and one sharper peak PI_90_NMP membrane. This suggests that the residual solvent remaining in the membrane might cause the side chain fluctuation and steric hindrance at the same time. In Figure 5b, the border peaks of PI_90_NMP suggested that the side chain mobility was promoted, resulting from the presence of remained solvent molecules. On the other hand, the sharper peak that appeared for PI_90_NMP revealed that some side chains were trapped because the local free volume was occupied by the solvent molecules. However, the proportion of trapped side chain seemed not too obvious by observing the intensity of the peak. Thus, it appears that the effect of residual solvent did not change the main structure of the membrane matrix, but it did affect the side chain mobility, causing the difference in kinetic energy. We suggested that the partial side chain mobility would be improved in the membrane which contained more residual solvent. This phenomenon was similar to that found in the report from Fu et al.,¹² which suggested that the existence of residual solvent should promote small segment motion.

3.3. Effect of Residual Solvent on Free Volume. Fractional Free Volume (FFV) and Fractional Accessible Volume (FAV). Figure 6 illustrates the FFV of PI_2880 and PI_90 series membranes during the MD duration of 1000 ps. It was observed that all the FFVs of the PI_2880 series membranes

TABLE 3: Energy Component in PI_2880 and PI_90 Series Membranes (kcal/mol)

casting solvent	intermolecular energy		intramolecular energy		total energy	
	PI_90	PI_2880	PI_90	PI_2880	PI_90	PI_2880
NMP	-6153.66	-6206.07	3074.64	3046.34	-3079.02	-3159.73
DMA	-4598.65	-4667.68	2727.28	2696.00	-1871.36	-1971.68
DIO	-5275.82	-5362.39	4439.55	4322.87	-836.267	-1039.52
THF	-4667.41	-4694.34	3434.47	3130.62	-1232.94	-1563.72
DIC	-3343.16	-3355.00	3140.80	3132.84	-202.362	-222.158

were higher than the FFVs of the PI_90 series. This could be attributed to the fact that the free spaces in the membranes would clearly be occupied by the residual solvent molecules, even though the segment motion might also donate some free space inside. The free volume in the PI membranes would be released by the solvent extracted from the membranes under the thermal treatment. The greater free volume in the PI_2880 series membranes is more favorable to gas sorption and permeation. This agrees well with the experimental results.¹³ To obtain the average FFV of the PI membranes during the dynamic structures, the FFV was obtained from the model selected by each 100 ps out of the 1000 ps duration. Ten sets of FFV data were chosen to obtain the average FFV of one membrane model. By estimating the difference in the average FFV between the PI_2880 and PI_90 series membranes, it was shown that the average FFV difference of PI membranes would improve when the difference in the quantity of solvent remaining in those membranes was higher. In other words, we found that the quantity of residual solvent dominated the FFV in the membrane in our present work.

Moreover, it was revealed that the differences among the PI_2880 series membranes fabricated from various casting solvents were less than those of the PI_90 series membranes. This is because the released free volume was mainly controlled by the amount and molar volume of solvent in the PI membranes. Meanwhile, the PI_2880 series membranes contained less solvent molecules. In this case, the values of different occupied spaces in the PI_2880 series membranes would be smaller than in the PI_90 series membranes, resulting in similar free volumes. Furthermore, it was shown that the tendency of FFV is opposite to the tendency of the boiling point of solvents. This is because solvents with lower boiling points in the membranes are removed more completely during the thermal treatment. Thus, the PI membranes

cast from lower boiling point solvents contained less residual solvent, which made it more possible to form the higher FFV.

However, it was also suggested that the membrane density might be increased due to the shrinkage of bulk volume caused by the evaporation of the solvent. The increasing membrane density was often accompanied with a reduction of free volume. Nevertheless, the highest weight percentage of residual solvent in the membranes in this study was only about 4.5%. It was considered that such low percentages of solvent could not have an effective influence on the whole polymer structure. Hence, it could be expected that the evaporation of residual solvent would improve the free volume in the membrane.

To analyze the effect on free volume in further depth, hard spherical particles with radius 1.83 Å (similar to the radius of N₂) were used to probe the FFV of five kinds of PI_90 and PI_2880 series membranes. The fractional accessible volume (FAV) was obtained from the probe. Furthermore, the relative FAV was adopted to discuss the effect of residual solvent on

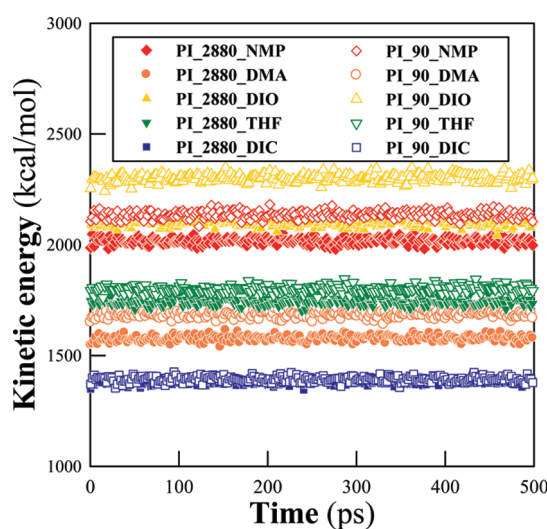


Figure 4. Kinetic energies of the PI_90 and PI_2880 membranes over 1000 ps.

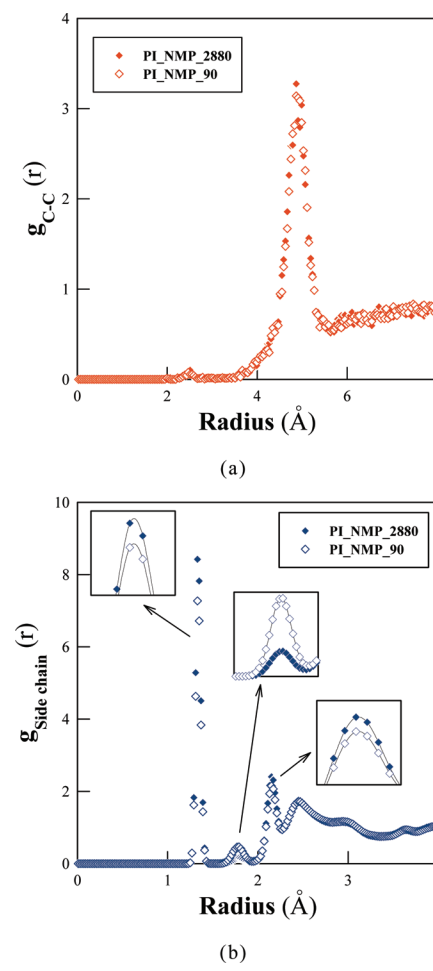


Figure 5. Radial distribution function of (a) C–C atom pairs and (b) side chain atoms in the PI_90_NMP and PI_2880_NMP membranes.

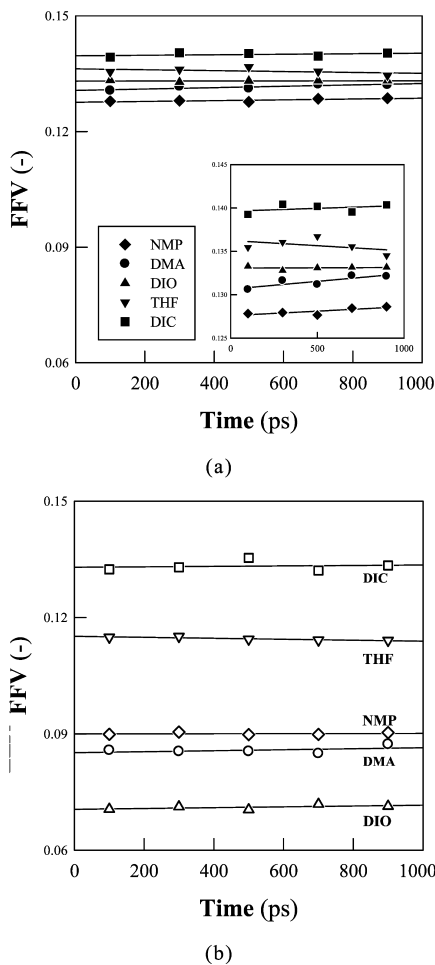


Figure 6. Fractional free volume of (a) PI_2880 and (b) PI_90 series membranes over MD of 1000 ps duration.

the accessible volume, where the relative FAV was calculated as follows:

$$\frac{\text{FAV(PI}_2880\text{)} - \text{FAV(PI}_90\text{)}}{\text{FAV(PI}_2880\text{)}} \times 100\%$$

Through the relative FAV analysis, the percentage of accessible volume released by the solvent evaporation was calculated. Figure 7 describes the relative FAV and gas permeability corresponding to the molar volume of the casting solvent. It was found that the relative FAV of PI membranes was significantly improved as the molar volume of the selected solvent increased. We can find the same tendency in the relative permeability, from past experimental work.¹³ This could be explained by the fact that the accessible or effective free volume for gas passing through the membrane would be more obviously increased when the extracted solvent had a larger molar volume.

Nevertheless, although the relative FAV analysis of the residual solvent effect in this study provides good performance for qualitative analysis, it still has some quantitative error. The reasons for the error could be explained as follows: (a) the size of the molecular model used in this study differs significantly from that of the real system due to the limitations of our present computational ability; (b) the hard spherical particles chosen here did not affect the interaction between the particle and membrane molecules; and (c) the selected force field might still produce some intrinsic error in the calculation process.^{26,27} In

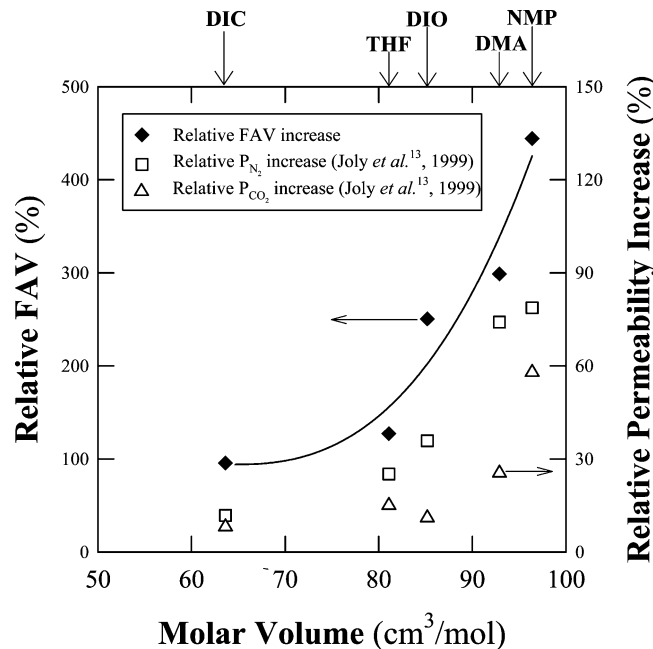


Figure 7. Relative fraction of accessible volume of PI membranes from this simulation work and the relative gas permeability of PI membranes from Joly et al.¹³

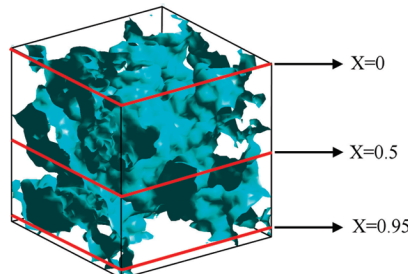


Figure 8. Selected cross sections of the molecular model in the x-direction.

addition to these, not all the released free volume detected here would really allow gaseous molecules to penetrate. Hence, it was necessary to analyze the free volume size distribution to further understand the residual solvent effect on membrane structure and gas transport behavior.

Free Volume Size Distribution Analysis. In our work, both qualitative and quantitative analyses of the free volume size distribution were used to investigate the free volume of PI membranes. In the qualitative analysis, three positions of membrane cross sections in the x-direction (as shown in Figure 8) were selected to analyze the free volume morphology. Figure 9 shows the cross-sectional images of five kinds of PI membranes in the x-direction. It shows that there was more free space in PI_2880 series membranes than in PI_90 series membranes. Moreover, the effect of residual solvent on the free volume became less pronounced when the differences in the residual solvent quantity and the solvent molar volume were lower (for instance, PI_THF and PI_DIC).

The cross-sectional images of molecular models in the x, y, and z directions were selected for the quantitative analysis. The equivalent diameter (D_{eq}) of the free area in the cross-sectional images was calculated by an image analysis technique in the Matlab program. Finally, the free volume size distribution was obtained by gathering the statistics of the counts and values of D_{eq} from the cross sections of membrane models.

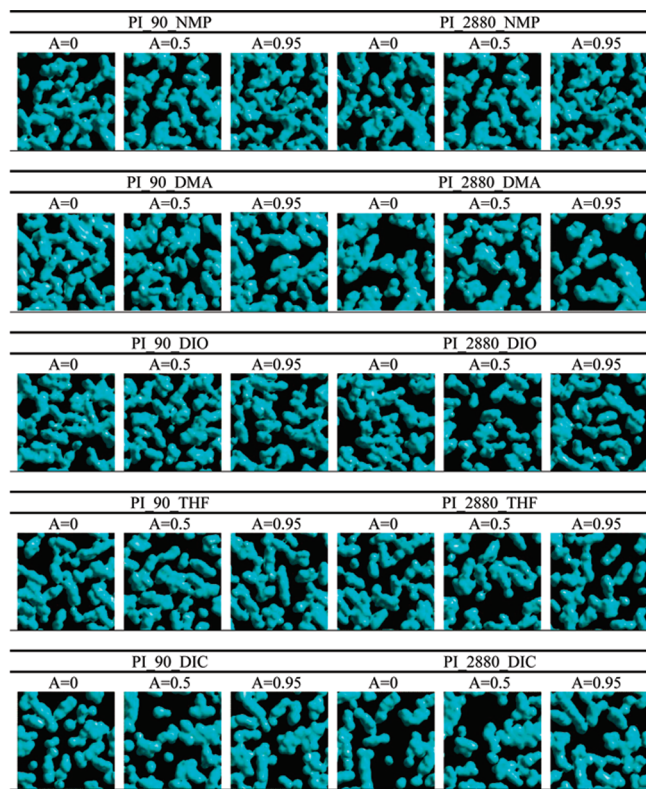


Figure 9. Free volume cross section of PI_NMP, PI_DMA, PI_THF, PI_DIO, PI_THF, and PI_DIC at thickness = 1.5 Å. ($A = x/a$, where a is the cell length in the amorphous model and x is the free volume cross section position in the x -direction).

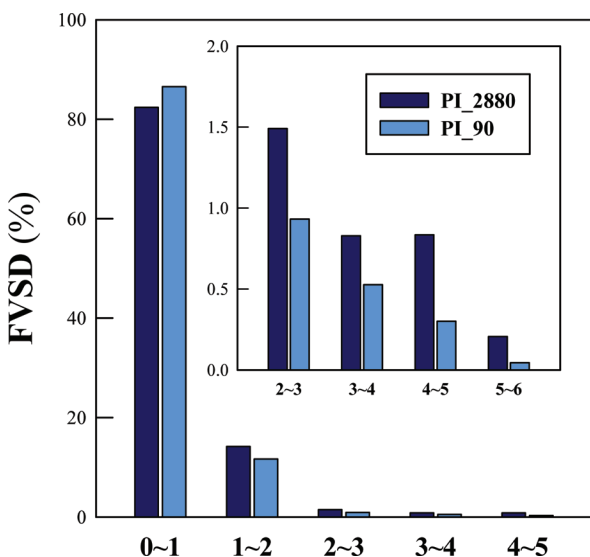


Figure 10. Free volume size distribution of PI_2880_NMP and PI_90_NMP membranes.

Figure 10 illustrates the effect of residual solvent quantity and molar volume on the free volume size distribution of the PI_2880_NMP and PI_90_NMP membranes. It was found that there was greater than 90% free volume in the range between 0 and 2 Å. This indicated that the 6FDA-mPDA PI membrane could be classified as a dense membrane for gas separation. Hence, the relatively larger and more continuous free space in this type of membrane would exert a great influence on its gas transport behaviors. Figure 10 shows that the PI_2880_NMP membrane had a higher percentage of free volume in the range of 3–6 Å in, while the PI_90_NMP membrane had a higher

TABLE 4: Percentage of Equivalent Diameters of Free Volume Counted in the PI_2880 and PI_90 Series Membranes during 3–6 Å (%)

casting solvent:	NMP	DMA	DIO	THF	DIC
PI_2880	1.87	1.47	2.04	1.76	1.03
PI_90	0.87	0.45	0.76	0.82	0.52
difference ^a	1.00	1.02	1.28	0.94	0.52

^a The difference is calculated as the percent of PI_2880 minus the percent of PI_90.

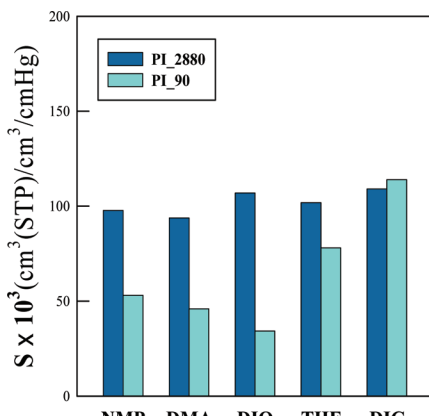
percentage of free volume between 0 and 1 Å. Similar results were also discovered for the PI_2880 and PI_90 series of the other membranes. This implied that the PI_2880 series membranes might contain more effective free volume for N₂ and O₂ passing through. Therefore, it could be suggested that the residual solvent apparently influenced the free volume size distribution, which affected the gas transport behaviors.

Table 4 lists the differences in the free volume sizes in the range of 3–6 Å between the PI_2880 and PI_90 series membranes cast from various casting solvents. Those differences had the same order (PI_DIO > PI_DMA > PI_NMP > PI_THF > PI_DIC) as the differences in the residual solvent quantities in the membranes. This shows that the effective free volume is indeed controlled by the solvent quantity, as we discussed above. Furthermore, we also found that the solvents with larger molar volume also tended to leave larger free volume after they were extracted from the membrane, such as NMP, DMA, and DIO. Meanwhile, the free volume size distribution was also compared with the gas solubility from the experimental data.¹³ The PI membranes showed higher differences in gas solubility coefficients when the differences in their effective free volume were larger, such as in PI_DIO and PI_DMA. This suggests that increasing the effective free volume benefits the sorption phenomenon after gas enters the membrane matrix.

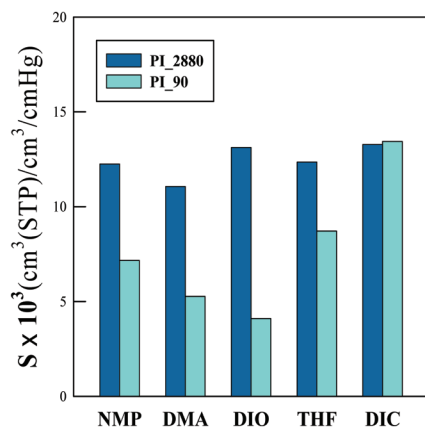
However, the gaseous molecules had lower diffusion ability in the PI_2880 series membranes with more effective free volume, as can be seen from the gas diffusion coefficients from the report of Joly et al.¹³ This shows that the gas transport in the membrane is affected by important factors besides the free volume distribution. Hence, the gas sorption behavior and diffusion mechanism were studied in order to further investigate the residual solvent effect.

3.4. Residual Solvent on Gas Transport Behavior. The gas transport in the polymeric membrane could be described as sorption and diffusion behavior by the solution-diffusion model. The residual solvent effect on the gas sorption behavior was analyzed and compared with the free volume distribution. Later, the gas diffusion mechanism was also studied to clarify the influence of residual solvent in the gas permeation.

Residual Solvent Effect on the Loading Gas Sorption. Figure 11a shows the effect of the residual solvent quantity on the N₂ solubility coefficient in the PI membranes. It was shown that the PI_2880 series membranes had noticeably higher solubility than the PI_90 series membranes. This could be attributed to the fact that the partial free spaces in the membrane would be released by the solvent evaporation processes. Meanwhile, those free spaces in the membranes enabled the gas to enter the membranes and find suitable free sorption sites. Moreover, the competition effect in sorption between gas and solvent molecules would be reduced when the solvent quantity in the membrane matrix decreased. Hence, a decrease of residual solvent in the membrane tended to encourage the gas solubility. In addition, the same result was observed in the case of the CO₂ solubility coefficient, as shown in Figure 11b. However,



(a)



(b)

Figure 11. Residual solvent effect on the solubility coefficients of (a) CO_2 and (b) N_2 on PI membranes cast from various casting solvents.

the effect of the residual solvent on gas sorption in the PI_90_NMP was the opposite. In this series, the solubility coefficient decreased when the residual solvent quantity decreased in the membrane. This could be explained by the fact that variations of residual solvent quantity and free volume in the PI_2880_DIC and PI_90_DIC membranes were rarely small, as can be seen by observing Tables 1 and 4. Hence, it could be suggested that only a limited amount of effective free volume was released during the solvent evaporation stage, which apparently did not effectively enlarge the gas sorption ability. It can be assumed that there should be other factors that control differences in the gas solubility of the PI_2880_DIC and PI_90_DIC membranes when their free volumes are quite similar. By comparing their intermolecular energies, it was found that the attractive energy between the gas and membrane–solvent matrix in the PI_90_DIC membrane was about 40 kcal/mol higher than that in the PI_2880_DIC membrane, which raised the possibility of more gaseous absorption in the PI_90_DIC membrane. Thus, it could be suggested that the gas sorption was affected by the effective free volume and the amount of residual solvent. When the free volumes are quite close, the sorption behavior would be dominated by the intermolecular attractive energy between the gas and membrane–solvent molecules.

Figure 11 also compares the sorption loading of N_2 and CO_2 in various PI membranes. It was found that the solubility coefficients of CO_2 in the PI membranes were about 7–10 times

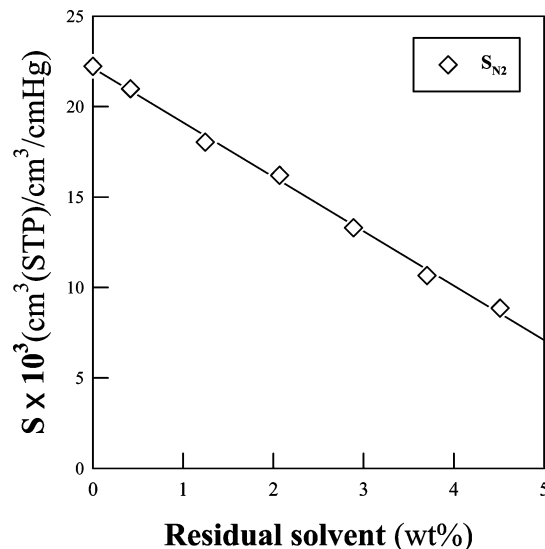


Figure 12. Residual solvent effect on the solubility of N_2 as a function of the amount of solvent molecules.

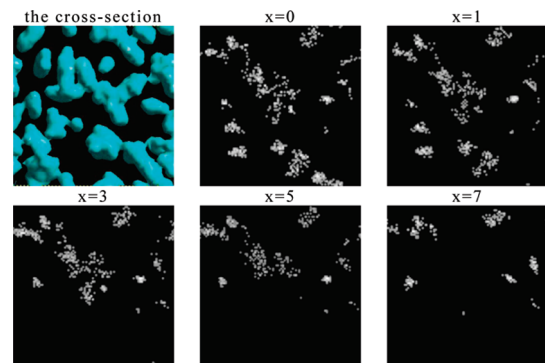


Figure 13. Mass distribution of nitrogen sorption sites on PI_2880_NMP and PI_90_NMP (where x is the number of solvent molecules in the membrane).

larger than the solubility coefficients of N_2 . This highlights that the sorption behavior between different gases in the PI membrane is well described by the molecular models we built in this study. In addition, the calculated gas solubility and selectivity coefficients in this study were compared with the experimental results.¹³ The simulated values obtained in this study revealed differences about 1–2 times those of the experimental data. By comparison with past studies, it was determined that the difference between simulated data and experimental data seems to be acceptable when the difference is less than a factor of 3–5.^{17,18}

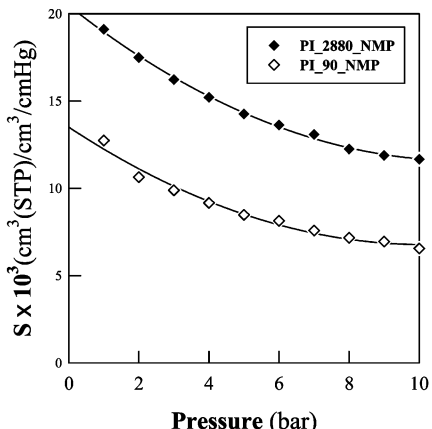
Figure 12 illustrates the effect of residual solvent quantity on the N_2 solubility coefficient in the PI_NMP membrane. It shows that the decrease of N_2 solubility was accompanied by an increase of residual solvent inside the membrane, even though the quantity of residual solvent remaining in the membranes is quiet low. Figure 13 shows the sorption sites of N_2 in PI membranes that contained various quantities of residual solvents. It also shows the effect of residual solvent quantity on gas sorption. The higher quantities of solvent in the membrane matrix provided fewer available sorption sites. Furthermore, it also indicated that the sorption sites of N_2 molecules were mainly located around the free volume margin.

Free Volume Distribution and Gas Sorption Loading. It was suggested by Joly et al.¹³ that differences in gas solubility of PI membranes might be attributed to the amount of residual solvent. However, the relation between the membrane free volume and

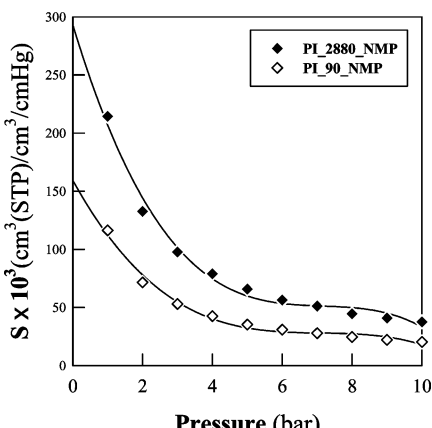
TABLE 5: Difference in Gas Solubility between the PI_90 and PI_2880 Series Membranes^a

	PI_NMP	PI_DMA	PI_DIO	PI_THF	PIDIC
N ₂	5.08	5.79	9.02	3.64	-0.16
CO ₂	44.72	47.88	72.71	23.77	-4.86

^a The difference is calculated as the solubility of PI_2880 minus the solubility of PI_90.



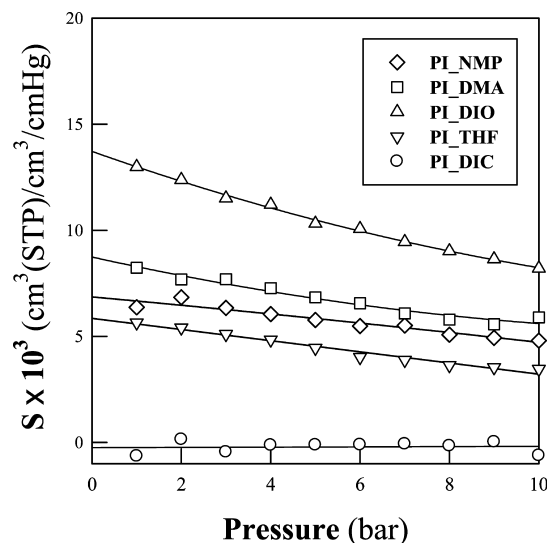
(a)



(b)

Figure 14. Solubilities of (a) N₂ and (b) CO₂ in the PI_2880_NMP and PI_90_NMP membranes at different pressures.

gas solubility was not discussed in their report. Therefore, the effective free volume in the PI membrane was compared with the gas solubility coefficient here. Table 5 lists the differences of N₂ and CO₂ solubility in the PI membranes, which were ordered as PI_DIO > PI_DMA > PI_NMP > PI_THF > PI_DIC. This tendency was consistent with the order of the effective

**Figure 15.** Difference of N₂ solubility between the PI_90 and PI_2880 series membranes under different pressures.

free volume differences (listed in Table 4). Therefore, it could be explained that the effective free volume in the membrane was conducive to the gas entering the membrane, thus leading to enhanced sorption behavior.

Effect of Operating Pressure on Gas Sorption Loading.

Figure 14 shows the effect of residual solvent on the sorption isotherms of N₂ and CO₂ in the PI_NMP membranes at different pressures. It shows that the solubility coefficient decreased noticeably when the operation pressure increased. The decrease in gas solubility might be caused by the saturation of the sorption sites at the higher pressure, which would not provide enough space for gas sorption. Furthermore, this tendency was generally more pronounced in the case of CO₂, which might result from the higher level interaction between CO₂ molecules and the membrane matrix. We found comparable results for PI membranes built from all the other casting solvents. Figure 15 describes the difference of N₂ solubility coefficient between PI_2880 and PI_90 series membranes constructed from casting solvents under different pressures. This analysis revealed that the residual solvent effect on gas solubility was reduced under higher pressures. Several reasons might explain the decrease in the solubility difference. First, the sorption sites for gaseous molecules might be occupied by the solvent molecules, which restrain the gas solubility. Meanwhile, the sorption sites competition would also be improved due to the significantly higher sorption loading at the higher pressure. Thus, the sorption sites would be saturated by the sorption behavior of gas and solvent molecules. Hence, the influence of residual solvent would also be relatively suppressed, due to the effect of gaseous

TABLE 6: Time Averaged Probability (%) of Various Transport Modes in the Case of N₂ and CO₂ Movement in the PI Membranes

	NMP		DMA		DIO		THF		DIC	
	PI_90	PI_2880								
P _{jump}	0.01	0.03	0.02	0.00	0.02	0.01	0.03	0.02	0.00	0.02
P _{trap}	1.84	1.48	1.41	1.11	2.04	1.84	1.48	1.41	1.11	2.04
P _{diffusive}	98.15	98.49	98.57	98.89	97.94	98.57	98.39	98.59	98.54	98.15
N ₂										
P _{jump}	0.00	0.00	0.00	0.00	0.00	0.00	0.00	0.00	0.00	0.00
P _{trap}	0.44	0.30	0.33	0.32	0.33	0.26	0.28	0.25	0.35	0.43
P _{diffusive}	99.56	99.70	99.67	99.68	99.67	99.74	99.72	99.75	99.65	99.57
CO ₂										
P _{jump}	0.00	0.00	0.00	0.00	0.00	0.00	0.00	0.00	0.00	0.00
P _{trap}	0.44	0.30	0.33	0.32	0.33	0.26	0.28	0.25	0.35	0.43
P _{diffusive}	99.56	99.70	99.67	99.68	99.67	99.74	99.72	99.75	99.65	99.57

competition on sorption. Furthermore, the residual solvent effect for the CO₂ sorption isotherms was similar to the case of N₂.

Effect of Residual Solvent on Gas Diffusion Probability.

The gas diffusion behavior in polymeric membranes was mainly dominated by the gaseous thermal motion inside. Those thermal motions could be classified as jumping, trapped motion, and diffusive motion, where the jumping and diffusive motion were considered as the effective thermal motions for the diffusion mechanism. Therefore, this study analyzed the effective thermal motions of N₂ and CO₂ in the PI membranes with various residual solvent quantities to understand the diffusion mechanism. Table 6 lists the thermal motion of gaseous N₂ molecules in the PI_2880 and PI_90 series membranes. It was shown that the effective thermal motion of N₂ molecules was reduced when the membrane had a lower quantity of residual solvent. This indicated that the fluctuation of molecules in the membrane would increase as the membrane contained more solvent molecules. However, the improvement of the thermal motion was not obvious, since free spaces in the membranes were occupied by the solvent molecules. Meanwhile, those solvent molecules remaining in the membrane would also form a barrier to gas movement. Thus, it was suggested that the small gaseous molecules in the membrane matrix might encourage partial segments motion but did not have a clear influence on the bulk structure. By the analysis of gas transport behavior, it was found that the residual solvent effect mainly affected the gas sorption phenomenon, not the gas diffusion mechanism.

4. Conclusions

The MD and MC techniques were used to investigate the effect of residual solvent on the free volume and gas transport behavior of the 6FDA-mPDA polyimide membranes. The free volume size distribution, gas sorption mechanism, and diffusion mechanism were discussed, and the conclusions can be summarized as follows. (1) From the energy and RDF analyses, the presence of residual solvent tends to promote the flexibility of polymer. (2) The free volume analysis shows that extracting the solvent has a greater effect on the free volume when the residual solvent has a larger molar volume and residual quantity. (3) The gas sorption behavior was mainly dominated by the effective free volume in the membrane. When the effective free volume is similar, the main factor becomes the intermolecular attractive energy. The effect of the residual solvent on the sorption behavior is eliminated at higher operation pressures due to the sorption competition between the gas and solvent molecules. (4) The effective thermal motion of gaseous molecules is improved in the higher residual solvent membranes, but it does not improve enough to control the gas transport behavior.

Thus, in summary, the residual solvent had a significant effect on the membrane free volume size distribution, and it changed the gas sorption behavior, which affected the gas permeability. The simulated results agreed well with the experimental data reported in the literature, suggesting that molecular simulations are a potential tool for material design and development of membrane applications.

Acknowledgment. We thank the Center-of-Excellence (COE) Program on Membrane Technology from the Ministry of Education (MOE), R.O.C., the project Toward Sustainable

Green Technology in the Chung Yuan Christian University (CYCU), Taiwan, and the National Science Council (NSC) for their financial support. Computational support from the National Center for High-Performance Computing, which provided the SGI O3800 computer and Cerius² software, is greatly appreciated.

References and Notes

- (1) Baker, R. W. *Membrane Technology and Applications*, 2 ed.; John Wiley & Sons: California, 2004.
- (2) Bi, J.; Simon, G. P.; Yamasaki, A.; Wang, C. L.; Kobayashi, Y.; Griesser, H. J. *Radiat. Phys. Chem.* **2000**, *58*, 563.
- (3) Hu, C. C.; Ruaan, R. C.; Lai, J. Y. *J. Chin. Inst. Chem. Eng.* **2003**, *34*, 101.
- (4) Bi, J. J.; Wang, C. L.; Kobayashi, Y.; Ogasawara, K.; Yamasaki, A. *J. Appl. Polym. Sci.* **2003**, *87*, 497.
- (5) Kruczak, B.; Matsuura, T. *J. Appl. Polym. Sci.* **2003**, *88*, 1100.
- (6) Shao, L.; Chung, T. S.; Wensley, G.; Goh, S. H.; Pramoda, K. P. *J. Membr. Sci.* **2004**, *244*, 77.
- (7) Hacarlioglu, P.; Toppare, L.; Yilmaz, L. *J. Appl. Polym. Sci.* **2003**, *90*, 776.
- (8) Brown, P. J.; East, G. C.; McIntyre, J. E. *Polym. Commun.* **1990**, *31*, 156.
- (9) Sakaguchi, Y.; Tokai, M.; Kawada, H.; Kato, Y. *Polym. J.* **1991**, *23*, 155.
- (10) Leblanc, N.; Le Cerf, D.; Chappay, C.; Langevin, D.; Métayer, M.; Muller, G. *Sep. Purif. Technol.* **2001**, *22–23*, 277.
- (11) Moe, M.; Koros, W. J.; Hoehn, H. H.; Husk, G. R. *J. Appl. Polym. Sci.* **1988**, *36*, 1833.
- (12) Fu, Y. J.; Hu, C. C.; Qui, H. Z.; Lee, K. R.; Lai, J. Y. *Sep. Purif. Technol.* **2008**, *62*, 175.
- (13) Joly, C.; Le Cerf, D.; Chappay, C.; Langevin, D.; Muller, G. *Sep. Purif. Technol.* **1999**, *16*, 47.
- (14) Smit, E.; Mulder, M. H. V.; Smolders, C. A.; Karrenbeld, H.; van Eerden, J.; Feil, D. J. *J. Membr. Sci.* **1992**, *73*, 247.
- (15) Gee, R. H.; Boyd, R. H. *Polymer* **1995**, *36*, 1435.
- (16) Yampolskii, Y. P.; Korikov, A. P.; Shantarovich, V. P.; Nagai, K.; Freeman, B. D.; Masuda, T.; Teraguchi, M.; Kwak, G. *Macromolecules* **2001**, *34*, 1788.
- (17) Hofmann, D.; Heuchel, M.; Yampolskii, Y.; Khotimskii, V.; Shantarovich, V. *Macromolecules* **2002**, *35*, 2129.
- (18) Hofmann, D.; Entrialgo-Castano, M.; Lerbret, A.; Heuchel, M.; Yampolskii, Y. *Macromolecules* **2003**, *36*, 8528.
- (19) Tung, K. L.; Lu, K. T. *J. Membr. Sci.* **2006**, *272*, 37.
- (20) Tung, K. L.; Lu, K. T.; Ruaan, R. C.; Lai, J. Y. *Desalination* **2006**, *192*, 391.
- (21) Tung, K. L.; Lu, K. T.; Ruaan, R. C.; Lai, J. Y. *Desalination* **2006**, *192*, 380.
- (22) Wang, X. Y.; Lee, K. M.; Lu, Y.; Stone, M. T.; Sanchez, I. C.; Freeman, B. D. *Polymer* **2004**, *45*, 3907.
- (23) Wang, X. Y.; in 't Veld, P. J.; Lu, Y.; Freeman, B. D.; Sanchez, I. C. *Polymer* **2005**, *46*, 9155.
- (24) Sedigh, M. G.; Onstot, W. J.; Xu, L.; Peng, W. L.; Tsotsis, T. T.; Sahimi, M. *J. Phys. Chem. A* **1998**, *102*, 8580.
- (25) Xiao, Y.; Chung, T. S.; Ching, M. L.; Tamai, S.; Yamaguchi, A. J. *Phys. Chem. B* **2005**, *109*, 18741.
- (26) Soldera, A. *Polymer* **2002**, *43*, 4269.
- (27) Lim, S. Y.; Tsotsis, T. T.; Sahimi, M. *J. Chem. Phys.* **2003**, *119*, 496.
- (28) Kim, T. H.; Koros, W. J.; Husk, G. R.; O'Brien, K. C. *J. Membr. Sci.* **1988**, *37*, 45.
- (29) Stern, S. A.; Mi, Y.; Yamamoto, H.; Clair, A. K. *J. Polym. Sci., Part B: Polym. Phys.* **1989**, *27*, 1887.
- (30) Hirayama, Y.; Yoshinaga, T.; Kusuki, Y.; Ninomiya, K.; Sakakibara, T.; Tamari, T. *J. Membr. Sci.* **1996**, *111*, 169.
- (31) Hirayama, Y.; Yoshinaga, T.; Kusuki, Y.; Ninomiya, K.; Sakakibara, T.; Tamari, T. *J. Membr. Sci.* **1996**, *111*, 183.
- (32) Wang, L.; Cao, Y.; Zhou, M.; Ding, X.; Liu, Q.; Yuan, Q. *Polym. Bull.* **2008**, *60*, 137.
- (33) Park, H. B.; Jung, C. H.; Lee, Y. M.; Hill, A. J.; Pas, S. J.; Mudie, S. T.; Wagner, E. V.; Freeman, B. D.; Cookson, D. J. *Science* **2007**, *318*, 254.
- (34) Low, B. T.; Xiao, Y.; Chung, T. S.; Liu, Y. *Macromolecules* **2008**, *41*, 1297.
- (35) Burns, R. L.; Koros, W. J. *Macromolecules* **2003**, *36*, 2374.